Published in final edited form as:
Biomaterials. 2011 December ; 32(36): 9612–9621. doi:10.1016/j.biomaterials.2011.09.012.

The influence of scaffold elasticity on germ layer specification of human embryonic stem cells

Janet Zoldan[1], **Emmanouil D. Karagiannis**[1], **Christopher Y. Lee**[2], **Daniel G. Anderson**[1,3,4], **Robert Langer**[1,3,4], and **Shulamit Levenberg**[5,*]

[1]H Koch Institute for Integrative Cancer Research, Massachusetts Institute of Technology, Cambridge, MA, USA

[2]Department of Biology, Massachusetts Institute of Technology, Cambridge MA, USA

[3]Harvard-MIT Division of Health Science and Technology, Massachusetts Institute of Technology, Cambridge, MA, USA

[4]Department of Chemical Engineering, Massachusetts Institute of Technology, Cambridge MA, USA

[5]Faculty of Biomedical Engineering, Technion, Haifa, Israel

Abstract

Mechanical forces are critical to embryogenesis, specifically, in the lineage-specification gastrulation phase, whereupon the embryo is transformed from a simple spherical ball of cells to a multi-layered organism, containing properly organized endoderm, mesoderm, and ectoderm germ layers. Several reports have proposed that such directed and coordinated movements of large cell collectives are driven by cellular responses to cell deformations and cell-generated forces. To better understand these environmental-induced cell changes, we have modeled the germ layer formation process by culturing human embryonic stem cells (hESCs) on three dimensional (3D) scaffolds with stiffness engineered to model that found in specific germ layers. We show that differentiation to each germ layer was promoted by a different stiffness threshold of the scaffolds, reminiscent of the forces exerted during the gastrulation process. The overall results suggest that three dimensional (3D) scaffolds can recapitulate the mechanical stimuli required for directing hESC differentiation and that these stimuli can play a significant role in determining hESC fate.

Introduction

Stem cell behaviour is correlated with cues that lie in their extracellular microenvironment[1, 2]. These cues operate on different spatial and temporal scales to pattern specific cellular responses that drive tissue morphogenesis and differentiation [3–5]

The mechanical properties of the extracellular microenvironment influence a variety of aspects of tissue behaviour. Studies of two dimensional (2D) cultures suggest substrate stiffness acts as a biomechanical regulatory factor in the tissue forming process. 2D substrate stiffness has been shown to control cell spreading and cytoskeleton assembly[6] as

*Corresponding Author: Shulamit Levenberg. Telephone: 972-4-829-4810; Fax: 972-4-829-4809; shulamit@bm.technion.ac.il.

well as directional motility[7]. In certain cell types, such as myotubes[8, 9] and mesenchymal stem cells[10], optimal differentiation was achieved on a substrate bearing the same stiffness as the natural microenvironment. Numerous stages of embryogenesis and fetal development are either affected by or generate mechanical forces [11]. More specifically, during gastrulation[11–13], blastula epiblast cells ingress[13, 14] and undergo changes in cell motility and shape, which affect the imposed cellular forces[11, 12, 15, 16]. The impact of these forces reflects both the mechanical characteristics acting on the cellular surfaces as well as the downstream intercellular signaling [17]. This crosstalk between the mechanical microenvironment and cell response, including cell induced matrix tension, can further create patterned mechanical stresses within embryonic tissues, impacting cell movement and differentiation[12, 18, 19].

The present work seeks to regulate hESC differentiation and assembly by manipulating mechanical forces acting on the environments in which they are cultured *in vitro*. The three dimensional (3D) scaffolds used provide a setting designed to foster self-assembly of components natural to tissue microenvironments [20], in general, and the utero-associated developing embryo environment, in particular[21]. In this manner, environmental mechanical forces acting upon cells can be manipulated by engineering the scaffold mechanical properties.

Materials and Methods

Scaffolds

Polymers—Poly(l-lactic acid) (PLLA) (Polysciences, Warrington, PA, *M*n~300,000) and poly(lactic co-glycolic acid) (PLGA) (Boehringer Ingelheim Resomer 503H, Ingelheim, Germany, *M*n~25,000) scaffolds (1:1) were prepared with varying proportions of low modulus poly(ε-caprolactone) (PCL) (Sigma Aldrich, *M*n~42,500), a rubbery crystalline polymer, or polyethylene glycol diacrylate (PEGDA) (Sigma Aldrich, St. Louis, MO, USA, Mn~575), a low molecular weight polymer.

Fabrication—All scaffolds were prepared using the salt-leaching technique (SL)[22]. Binary PLLA/PLGA and ternary PLLA/PLGA/PCL scaffolds were prepared by dissolving the designated polymers at selected weight ratios (Table 1) in chloroform to yield 5% (w/v) polymer solutions. PLGA/PLLA/PEGDA scaffolds were formed by crosslinking PEGDA with benzoyl peroxide (Sigma Aldrich). A single PEGDA concentration was used, while benzoyl peroxide (BP) concentrations were varied (1% and 0.05% w/v). PLLA and PLGA (1:1) were dissolved at 50mg/ml in dichloroethane, followed by addition of PEGDA and BP. The solution was then loaded into molds packed with sodium chloride particles (212–500 μm) and heated at 55^0C for 8 hours until solidification. Thereafter, the sodium chloride was leached out to create a sponge via water immersion.

Scaffold characterization

Morphology

Scaffold morphology was analyzed using a Philips XL-30 scanning electron microscope (SEM) and a Zeiss LEO982 high-resolution scanning electron microscope (HRSEM). Images of secondary electrons were generated at accelerating voltages of 10KV and 2KV, respectively. The samples were gold sputtered to create a ~50nm-thick conductive layer. Seeded scaffolds were imaged by light microscopy (Axiovert 200, Carl Zeiss) every other day over the 14-day culturing period to characterize cell density, matrigel coating integrity and scaffold shape.

Porosity

Scaffold porosity was measured using an AutoPore IV 9500 (Micromeritics, Norcross, GA, USA) by applying various degrees of pressure (≤50 psi) to scaffolds immersed in mercury. The pressure required to introduce mercury into scaffold pores is inversely proportional to the size of the pores. Porosity for each scaffold was calculated as the mean of three samples.

Mechanical properties

Sample tensile testing was determined on samples of 10mm X 15mm X 1mm (w X h X t) using an Instron 5544 (Instron, Canton, MA, USA) at a strain rate of 0.01 mm/s until failure was reached. The elastic modulus was calculated as the slope of the linear portion of the stress-strain curve. The ultimate tensile strength was determined as the maximum point in the stress-strain curve.

Cell Culture

Human ESCs (H9 clone) were grown on a human foreskin fibroblast (ATCC) feeder layer in knockout media as previously described[23]. Cell differentiation was induced by transferring hESCs to 15cm petri dishes to allow for embryoid body (EB) formation. EB formation began in EB media (80% knock-out DMEM, 20% knock-out serum, 1mM glutamine, 0.1mM beta mercaptoethanol and 1% non-essential amino acids) suspension and yielded approximately 3×10^6 cells per plate[24]. After 8 days in culture, EBs were dissociated by trypsinization and seeded (~2×10^6 cells per $5\times5\times1mm^3$) on selected scaffolds. To facilitate cell attachment to the scaffolds, hESCs were mixed with matrigel solution (BD Biosciences, San Jose, CA, USA) before being loaded onto the scaffolds[22, 24]. The gel mixture solidified at 37°C and allowed for cell retention within the scaffolds. Scaffolds seeded with hESCs were grown in 2 ml media under gentle shaking conditions.

In parallel, EBs were grown for 22 days as controls for quantitative PCR. Half of the media volume was changed every 2–3 days and EBs were passaged once a week.

Quantitative PCR

After two weeks in culture, hESC-embedded scaffolds were homogenized using iron beads and Mini Bead Beater™ (Biospec Products) and total RNA was extracted using an RNEasy mini kit (Qiagen, Catsworth, CA, USA). Crude isolated RNA (100–500 ng) was reverse transcribed with SuperScript III First-Strand system (Invitrogen, Chicago, IL, USA). cDNA aliquots equivalent to 90 ng of total RNA were amplified with Taq Polymerase and Step One Plus Real time PCR System (Applied Biosystems, Chicago, IL, USA) according to standard protocols. Quantified gene expression values were normalized against GAPDH gene expression, where normalized expression = $2^{[-(Ctsample - CtGAPDH]}$. The mean minimal cycle threshold values (Ct) was calculated from quadruplicate samples performed in each of the three independent experiments. After normalization, gene expression plots were prepared, presenting values relative to gene expression in EBs grown in suspension for the same interval of time. Human ESC differentiation to each of the three germ layers (endoderm, ectoderm and mesoderm) on the various tested scaffolds was evaluated by expression of selected genes (summarized in Supplementary Table 1).

To provide a more comprehensive assessment of the scaffold stiffness-germ layer-specific gene expression correlation, we monitored a wide range of marker genes using TaqMan® Array Custom Micro Fluidic Card (TaqMan® human Stem Cell Pluripotency Array) specifically designed to monitor human embryonic stem cell differentiation pathways as well as pluripotency. Select hESC embedded scaffolds were grown for 1 week or 2 weeks in culture and then processed as described above. cDNA samples (1000ng) were premixed with

TaqMan® Universal PCR Master Mix (with AmpErase® UNG)and loaded onto the TaqMan Array card. Gene amplification was performed with Applied Biosysytems 7900HT Fast Real-Time[25] PCR System according to manufacturer instructions. Analysis of the TaqMan® Array Micro Fluidic Card was performed with SDS Software v2.4 (Applied Biosysytems). Quantified gene expression values were normalized against GAPDH gene expression. To analyze the effect of 3D scaffolds on hESC differentiation, normalized gene expression values were presented as relative values to gene expression in EBs grown in suspension for the same interval of time.

Immunohistochemisatry

hESC seeded scaffolds were cultured for 2 weeks, then fixed for 6h in 10% formalin and paraffin embedded. Immunohistochemical staining was carried out by using the Biocare Medical Universal HRP-DAB kit (Biocare Medical, Walnut Creek, CA) according to the manufacturer's instructions, with prior heat treatment at 90°C for 20 min in ReVeal buffer (Biocare Medical) for epitope recovery. The primary antibodies were: KDR (1:20; Santa Cruz Biotechnology, Santa Cruz, CA, USA.), brachyury (1:50; R&D, Minneapolis, MN, USA), vimentin (1:50; Dako, Carpinteria, CA), CD31 (1:20; Dako), trophonin (1:200; R&D), collagen1 (1:200) (mesoderm representative), SOX17 (1:40; R&D), MIXL1 (1:40; R&D), GCG (1:3000; Sigma-Aldrich, Atlanta, GA), PDX1(1:2000; Abcam, Cambridge MA) (endoderm representative), SOX1(1:40; R&D), ZIC1 (1:40; R&D), nestin (1:100; BD Biosciences, San Jose, CA), PAX6 (1:200; Abcam), HLXB9 (1:50; Abcam) (ectoderm representative). Overlapping microscopic pictures were taken at a magnification of 100X and 40X so that the entire area of the sample was covered (ExioVert200, Carl Ziess). Imaging software (ImageJ, NIH) was used to determine the % area stained positively for specific antibody out of the total sample area[26].

Gene clustering and protein mapping

To evaluate expression patterns during culture on the 3D scaffolds of variable elasticity we performed hierarchical clustering analysis of the expressed genes. Specifically, we computed the pairwise Euclidean distances between the different expression levels of the 96 genes in the various samples. Then, from these Euclidian distances we constructed an agglomerative hierarchical cluster tree. The resulting analysis was visualized as a heat map with the genes clustered according to the calculated distances. To identify the functionality of gene clusters, we first expanded the data sets by identifying primary interaction partners of the genes and constructed protein-protein interaction networks. We then identified the functionality of the extended networks by assigning Gene Ontology attributes to the networks. To expand the networks we performed the analysis using the GeneMania algorithm in the Cytoscape platform. To assign Gene Ontology attributes we utilized the BiNGO algorithm within the same platform.

Statistical Analysis

To take multiple comparisons into account, analysis of variance (ANOVA) was performed, using InStat software (GraphPad). Statistical significance was set as $p<0.05$.

Results and Discussion

To characterize differentiation in various 3D environments, hESCs were grown on scaffolds of elastic moduli ranging from 0.05–7 MPa (Fig. 1 and Data S1). This range of moduli was chosen to better fit the modulus of various tissues[27] that arise from the three germ layers. Elasticity was manipulated by preparing scaffolds of binary poly-L-lactide acid (PLLA) and copolylactic/glycolic acid (PLGA) blends at varying ratios, or by diversifying the type

(polycaprolactone, (PCL) or polyethylene glycol diacrylate, (PEGDA)) and quantity of polymer supplementing the basic 1:1 PLLA/PLGA scaffold composite (Fig. 1, Supplementary Data1 and Supplementary Fig. 1 summarize scaffold characterization).

In an effort to draw correlative associations between scaffold stiffness and hESC differentiation, gene expression unique to each of the three germ layers was quantified after 14 days in culture (Supplementary Table 1 and Supplementary Data 2). Four groups of scaffolds were categorized, each with a distinct elasticity range and gene expression pattern. In general, hESCs cultured on scaffolds of >6MPa stiffness (ternary PEGDA-containing scaffolds), remained non-differentiated and exhibited reduced expression of the majority of the tested germ layer-specific genes (Fig. 2a–c and Supplementary Fig 2). In contrast, high elastic modulus (HiEM) scaffolds (1.5–6MPa; neat PLLA or high PLLA content supplementing binary PLLA/PLGA scaffolds) promoted mesodermal differentiation, as exhibited by increased expression of the FOXF1, MEOX1 and KDR genes (Fig. 2a). FOXF1 and MEOX1 underwent 80- and 30-fold increases in expression levels, respectively, among cells cultured on neat PLLA scaffolds, when compared to those grown in suspension. No endoderm- or ectoderm-associated gene expression (Fig. 3b**,** c) was detected, further confirming mesodermal formation in these environments.

Intermediate elastic modulus (IntEM) scaffolds (0.1–1MPa; low PLLA-content binary and ternary scaffolds supplemented with 20% PCL) promoted elevated (2–3-fold) endoderm-specific gene expression of GSC and SOX17, when compared to high elastic modulus (HiEM) scaffolds (Fig. 2b), paralleled with reduced expression of mesoderm-related genes. In addition, the embedded hESCs expressed high levels of brachyury and MIXL1, both associated with the primitive streak early gastrulation phase. Elevated gene expression of brachyury and MIXL1 has also been described for mouse ESCs cultured in 2D environments within this stiffness range [28]. Thus, as scaffold modulus increases, cells undergo a transition from primitive streak structures to mesoderm layers. To further confirm this, protein expression level of selected markers was compared between HiEM $PLLA_{75}/PLGA_{25}$ and IntEM $PLLA_{25}/PLGA_{75}$ scaffolds by performing immunoassays (Supplementary Fig. 3). On both scaffolds no expression of ectodermal markers SOX1 and ZIC1 was detected. The HiEM $PLLA_{75}/PLGA_{25}$ scaffold exhibited 35% expression of mesodermal marker KDR and 30% of primitive streak marker brachyury, but no expression of MIXL1 and SOX17 endodermal markers. On the other hand, the IntEM $PLLA_{25}/PLGA_{75}$ scaffold had no expression of mesodermal KDR marker coupled with high expression levels of endoodermal markers SOX17 (41%) and primitive streak markers MIXL1 (62%) and brachyury (74%). In summary, protein expression is mirrored by gene expression patterns. In addition, despite variances in chemical composition, scaffolds providing similar degrees of scaffold elasticity induce comparable gene expression profiles.

Further reduction of scaffold elastic modulus (LoEM; <0.1MPa; neat PLGA, neat PCL or ternary scaffolds supplemented with 80% PCL) resulted in increased expression of the SOX1 and ZIC1 ectodermal germ layer-associated genes, along with suppression of mesodermal-specific gene expression (Fig. 2c). hESCs grown on $[PLLA_{50}/PLGA_{50}]_{20}/PCL_{80}$ scaffolds exhibited a 25- and 15-fold increase in ectodermal SOX1 and ZIC1 genes, respectively, while expression of the FOXF1, MEOX1 KDR mesodermal genes and the brachyury premesodermal gene were reduced by 50–70% in comparison to embryonic bodies (EBs) grown in suspension

Differences in scaffold composition did not affect scaffold morphology or porosity (Fig. 1). In addition, application of a matrigel coating (optimized to ~ 5μm thickness) maintained uniform scaffold surface chemistry regardless of scaffold composition. It has been reported that cells can sense and respond to the stiffness of substrates under gels of 10–20μm

thickness[29]. In addition, compositional differences leading to divergent scaffold degradation rates were unlikely to influence hESC differentiation, as variances in such degradation were not manifested within the time frame of these experiments (Supplementary Fig. 1). These data then indicate that the modulus of the 3D environment can direct differentiation of hES cells embedded within.

We hypothesize that scaffold stiffness may mimic natural forces experienced during gastrulation-related cell movement, ultimately directing cell differentiation. Gastrulation usually occurs within 14–21 days, which falls within the time frame of the *in vitro* experiments performed herein. Throughout this process, epiblast cells converge at the midline before ingressing at the primitive streak[13]. However, the rate of cell movement along the top of the blastula exceeds that of ingression, thereby leading to compression of epiblast cells into bottle-shaped cells at the primitive streak[13]. The cells first to ingress form the endoderm, while the mesoderm arises from those ingressing and migrating at a later stage. The ectoderm then develops from those cells remaining at the surface. Thus, we hypothesize that both endoderm- and mesoderm-forming cells experience increased mechanical forces during their ingression through the primitive streak before reaching their final destination. The present results demonstrate that increased scaffold stiffness indeed facilitates differentiation into endodermal and mesodermal germ layers, when compared to that required to trigger ectoderm formation. As stiffness increases, endodermal differentiation is suppressed and mesodermal differentiation is favored. Indeed, mesodermal cells exert greater tensional forces than epithelial cells[30]. However, upon reaching a specific elasticity threshold, cells fail to respond and remain undifferentiated.

To provide a more comprehensive assessment of the correlation between scaffold stiffness and germ layer-specific gene expression, we monitored a wide range of marker genes using the TaqMan® human Stem Cell Pluripotency Array (Applied Biosystems). The 96 genes were categorized by those representing specific germ layers (Fig. 3a–c), trophoblasts or degree of stemness (Supplementary Fig. 4). The broad-range gene analysis of cells cultured for two weeks and their protein expression levels (Fig 3d–f), further supported our findings suggesting an impact of scaffold stiffness on hESC differentiation, where HiEM scaffolds favored mesodermal differentiation, IntEM scaffolds led to endodermal differentiation and LoEM scaffolds to ectodermal differentiation. Elevated expression (1.5–6-fold) of ectodermal differentiation was only detected on the $[PLLA_{50}/PLGA_{50}]_{20}/PCL_{80}$ and neat PLGA LoEM scaffolds (Fig. 3a). This family of elevated ectodermal genes can be further subcategorized to those related to neuroepithelial cells (PAX6, nestin and FOXD3) or motor neurons (HLXB9)[31, 32], suggesting propagation of a mixture of these cell types on LoEM scaffolds after two weeks in culture.

Upon analysis of endodermal differentiation (Fig 3b), all markers (apart from the mature hepatic TAT marker and hepatic endocrine precursors markers PTF1A and IAPP) were upregulated in the hESC-embedded IntEM $PLLA_{50}/PLGA_{50}$ and $PLLA_{25}/PLGA_{75}$ scaffolds, in sharp contrast to their levels detected in HiEM $PLLA_{75}/PLGA_{25}$ or LoEM $[PLLA_{50}/PLGA_{50}]_{20}/PCL_{80}$ and neat PLGA scaffolds. The study was then broadened to evaluate the status of immature endodermal markers, such as those linked with the extraembryonic endoderm. Such cellular states, typically present prior to mammalian gastrulation, further progress to form the visceral endoderm (AFP, SERPINA1) and the parietal endoderm (LAMC1, LAMA1)[33, 34]. All tested extraembryonic lineage markers (AFP, SERPINA1, LAMC1, LAMB1, LAMA1, FN1, SOX17, FOXA2 and GATA4) were upregulated 2–8-fold in both IntEM scaffolds tested.

Morphogenesis of the primitive gut tube, formed from definitive endoderm cells, gives rise to gut organs, including the liver and pancreas [35]. Thus, signs of mature endoderm

derivatives were also sought out in hESC-embedded IntEM scaffolds. AFP and SERPINA1, both early markers of hepatocyte presence, were upregulated 4–6-fold in IntEM scaffolds, while TAT, representing a more mature hepatocyte state, was not expressed at all. Pancreatic differentiation within hESC-embedded $PLLA_{50}/PLGA_{50}$ scaffolds was observed, as expressed by upregulation of mature pancreatic markers (SST: 6-fold, INS: 19-fold, GCG: 10-fold). In contrast, hESC grown on $PLLA_{25}/PLGA_{75}$ IntEM scaffolds exhibited a 3-fold upregulation of the PAX4 early pancreatic endoderm marker and a 5-fold upregulation of the IPF1 (PDX1) early gut endoderm marker, while expression of mature markers was absent.

In contrast, mesoderm-related genes were most upregulated among hESCs grown on either HiEM $PLLA_{75}/PLGA_{25}$ scaffolds or on IntEM $PLLA_{50}/PLGA_{50}$ scaffolds (Fig 3c). Genes related to the lateral, intermediate and dorsal mesodermal zones[36] were detected in these scaffolds within two weeks of incubation. Markers of functional mesoderm-derived cells, such as cardiomyocytes (ACTC:3.5-fold in $PLLA_{75}/PLGA_{25}$), and endothelial/vascular cells (CD34, PECAM1, CDH5), were upregulated (5–15fold) in cells grown on these scaffolds, while the HBB and HBZ blood markers were absent. Similarly, the WT1 urogenital marker was upregulated by 13.4- and 1.75-fold in the $PLLA_{50}/PLGA_{50}$ and $PLLA_{75}/PLGA_{25}$ scaffolds, respectively. These same scaffolds featured dorsal mesoderm differentiation to skeletal muscle (MYOD1, DES), early (RUNX2) and mature (COL1A1) osteoblasts and chondrocytes (COL2A1). These findings fall in line with the reported increase in osteogenic differentiation of mouse ESCs on 2D substrates of stiffness similar to that of $PLLA_{75}/PLGA_{25}$ [28].

To examine gene expression kinetics and to shed light on the progression of hESC differentiation over the 2-week culture period, cell differentiation within 3D scaffolds cultured for one week was also analyzed (Supplementary Fig. 5). An identical correlation between gene expression patterns and germ layer differentiation and scaffold stiffness was seen, as was cell population makeup within scaffolds, albeit at a less mature state than that of 2-week cultures. The degree to which the mechanical properties of the scaffolds direct hESC differentiation was further assessed by seeding scaffolds with hESCs of varying differentiation statuses (Supplementary Fig. 6). The differentiation fate of EB day 4, 8 and 15 seeded on $PLLA_{50}/PLGA_{50}$ scaffolds was monitored. All cell-embedded scaffolds exhibited similar gene patterning after two week in culture, with ectodermal gene downregulation in all samples, regardless of the initial differentiation state of hESC at seeding. This indicates that mechanical microenvironmental cues direct stem cell differentiation and overcome variances between precursor populations.

To further evaluate the gene expression patterns after two weeks of cell culture on the 3D scaffolds, we performed hierarchical clustering analysis of the expressed genes, visualized as a heat map (Figure 4a). From the analysis we identified clusters of genes that are uniquely upregulated in hESC grown on either LoEM or InEM or HiEM matrices (Figure 4b). To identify the significance of these sets of genes, we examined their functionality in the context of a developmental process and cell differentiation in the following manner. First we expanded the gene data sets by identifying primary interaction partners of the genes and constructed protein-protein interaction networks that suggest pathways associated with these genes (Figure 4c). From these pathways we then infer the function of the extended networks by assigning Gene Ontology[37] attributes to the networks (using GeneMania algorithm[38] in the Cytoscape platform[39] and BiNGO algorithm[40] within the same platform)(Figure 4d). By doing so we identified biological processes that are driven by the sets of genes that include or are closely related to the genes that are upregulated in hESCs cultured on the different matrices. The Gene Ontology analysis revealed that genes upregulated in hESCs grown on LoEM correlate with trophoectoderm development, anterior/posterior axis

specification, stem cell maintenance and neurogenesis; genes upregulated in hESCs grown on InEM correlated with endodermal tissue morphogenesis (such as digestive system, exocrine system, lungs, and epithelium); and genes upregulated in hESCs grown on HiEM correlate with mesodermal tissue morphogenesis (muscle, blood vessels, heart, cartilage and bone). Thus we performed a more constricted analysis taking into account that clusters of genes are uniquely upregulated in concert instead of analyzing the function of each gene separately (performed in Figure 3). However, both analyses yield the same correlations between germ layer differentiation and scaffold elasticity.

The broad-range gene analysis described here further supports our findings suggesting an impact of scaffold stiffness on hESC differentiation, where high, intermediate and low elastic moduli promoted mesodermal, endodermal and ectodermal differentiation, respectively. In this manner, substrate stiffness acts as an external source of signaling between cells within a common environment. The molecular mechanisms linking scaffold stiffness and hESC differentiation remain to be explored. Previous work has focused on the impact of stiffness on differentiation (21–25), but involved models of more mature cells than the highly pluripotent hESCs, thereby complicating any attempt at comparing the signaling events with those of the present report. One potential way in which mechanical properties could influence development is by passively constraining the movement of tissues and cells. Cells tend to move more slowly and exert higher tractions forces on stiffer 2D substrates as well as increase their cortical stiffness by changing the amount and pattern of polymerized cytoskeletal actin[11, 17, 41]. In the xenopus embryo, cell-to-cell interactions have been shown to determine cytoskeleton assembly by controlling the amount of cadherin expressed on the cell surface[42]. Constraint of cell movement occurs during gastrulation[13]. Gastrualtion starts by the convergence of epiblast cells at the midline followed by their ingression at the primitive streak. However, these cells move along the top faster than they can separate off and move internally, leading to compression of epiblast cells into bottle shaped cells at the primitive streak[13]. These cells then loose their E-cadherin cell-cell adhesion[43] and leave the primitive streak. Changes in cell shape lead presumably to changes in actin assembly and cell-to-cell interactions, which in turn regulated cadherin expression (similar to observations in the xenopus embryo)[42]. If the 3D scaffold microenvironment mimics gastrulation-like cell constraints, then it can be proposed that equivalent cellular displacement is maintained regardless of scaffold modulus(as was shown for kidney epithelial cells regulating forces by maintaining a state of constant deformations[44]). Thus the variations in scaffold modulus will be manifested as variations in the forces exerted by the embedded cells. We hypothesize that cells grown on stiffer scaffolds may respond to higher counterforces by activating the relevant differentiation routes. More specifically, mesodermal differentiation might require higher intercellular forces than endoderm, which might require higher intercellular forces than ectoderm. This model resembles the hierarchy of germ layer single-cell adhesion forces reported in zebrafish[45] and cell aggregate surface tensions measured in chick embryos[30, 46]. However, to date, minimal research has been conducted in pursuit of human embryonic germ layer mechanical properties. Another possibility is that cells exert similar forces on the various scaffolds but smaller displacements during differentiation on stiffer scaffolds. By doing so, cell-cell interactions would be affected and trigger differentiation to a certain germ layer. Whether uniform cell displacement or uniform mechanical forces lie at the base of directed differentiation is yet to be answered. Nevertheless, the net effect of these mechanisms demonstrates a direct correlation between scaffold stiffness and control of hESC differentiation.

Conclusions

The work in this report demonstrates that hESC differentiation can be directed to each of the three germ layers by engineering their physical microenvironment. Through a broad range of gene analysis and protein expression, we show that scaffolds can provide controlled mechanical stimuli required for directing hESC differentiation *in vitro* into each of the three germ layers. Differentiation to each germ layer was promoted by a different stiffness threshold of the scaffolds, reminiscent of the forces exerted during the gastrulation process.

3D scaffolds recapitulating these mechanical cues may allow for the study of the role of mechanotransduction in early embryonic development, and pave the way for generating specific cell type-enriched populations for regenerative medicine applications.

Supplementary Material

Refer to Web version on PubMed Central for supplementary material.

Acknowledgments

The authors would like to thank Yehudit Posen for her contribution in editing the paper. This research was supported by Israel Science Foundation (F.I.R.S.T program) and NIH grants DE-016516 and HL-060435.

References

1. Discher DE, Mooney DJ, Zandstra PW. Growth factors, matrices, and forces combine and control stem cells. Science. 2009; 324(5935):1673–7. [PubMed: 19556500]
2. Guilak F, Cohen DM, Estes BT, Gimble JM, Liedtke W, Chen CS. Control of stem cell fate by physical interactions with the extracellular matrix. Cell Stem Cell. 2009; 5(1):17–26. [PubMed: 19570510]
3. Langer R, Vacanti JP. Tissue engineering. Science. 1993; 260(5110):920–6. [PubMed: 8493529]
4. Wobus AM, Boheler KR. Embryonic stem cells: prospects for developmental biology and cell therapy. Physiol Rev. 2005; 85(2):635–78. [PubMed: 15788707]
5. Keller G. Embryonic stem cell differentiation: emergence of a new era in biology and medicine. Genes Dev. 2005; 19(10):1129–55. [PubMed: 15905405]
6. Georges PC, Janmey PA. Cell type-specific response to growth on soft materials. J Appl Physiol. 2005; 98(4):1547–53. [PubMed: 15772065]
7. Pelham RJ Jr, Wang Y. Cell locomotion and focal adhesions are regulated by substrate flexibility. Proc Natl Acad Sci U S A. 1997; 94(25):13661–5. [PubMed: 9391082]
8. Engler AJ, Griffin MA, Sen S, Bonnemann CG, Sweeney HL, Discher DE. Myotubes differentiate optimally on substrates with tissue-like stiffness: pathological implications for soft or stiff microenvironments. J Cell Biol. 2004; 166(6):877–87. [PubMed: 15364962]
9. Levy-Mishali M, Zoldan J, Levenberg S. Effect of scaffold stiffness on myoblast differentiation. Tissue Eng Part A. 2009; 15(4):935–44. [PubMed: 18821844]
10. Engler AJ, Sen S, Sweeney HL, Discher DE. Matrix elasticity directs stem cell lineage specification. Cell. 2006; 126(4):677–89. [PubMed: 16923388]
11. Ingber DE. Mechanical control of tissue morphogenesis during embryological development. Int J Dev Biol. 2006; 50(2–3):255–66. [PubMed: 16479493]
12. Beloussov LV, Grabovsky VI. Morphomechanics: goals, basic experiments and models. Int J Dev Biol. 2006; 50(2–3):81–92. [PubMed: 16479477]
13. Keller R, Davidson LA, Shook DR. How we are shaped: the biomechanics of gastrulation. Differentiation. 2003; 71(3):171–205. [PubMed: 12694202]
14. Gadue P, Huber TL, Nostro MC, Kattman S, Keller GM. Germ layer induction from embryonic stem cells. Exp Hematol. 2005; 33(9):955–64. [PubMed: 16140142]

15. Odell GM, Oster G, Alberch P, Burnside B. The mechanical basis of morphogenesis. I. Epithelial folding and invagination. Dev Biol. 1981; 85(2):446–62. [PubMed: 7196351]
16. Farge E. Mechanical induction of Twist in the Drosophila foregut/stomodeal primordium. Curr Biol. 2003; 13(16):1365–77. [PubMed: 12932320]
17. von Dassow M, Davidson LA. Variation and robustness of the mechanics of gastrulation: the role of tissue mechanical properties during morphogenesis. Birth Defects Res C Embryo Today. 2007; 81(4):253–69. [PubMed: 18228257]
18. Stern CD. A simple model for early morphogenesis. J Theor Biol. 1984; 107(2):229–42. [PubMed: 6325826]
19. Beloussov LV, Luchinskaya NN, Ermakov AS, Glagoleva NS. Gastrulation in amphibian embryos, regarded as a succession of biomechanical feedback events. Int J Dev Biol. 2006; 50(2–3):113–22. [PubMed: 16479480]
20. Goodbye flat biology? Nature. 2003; 424(6951):861.
21. Adissu HA, Asem EK, Lelievre SA. Three-dimensional cell culture to model epithelia in the female reproductive system. Reprod Sci. 2007; 14(8 Suppl):11–9. [PubMed: 18089605]
22. Levenberg S, Golub JS, Amit M, Itskovitz-Eldor J, Langer R. Endothelial cells derived from human embryonic stem cells. Proc Natl Acad Sci U S A. 2002; 99(7):4391–6. [PubMed: 11917100]
23. Amit M, Margulets V, Segev H, Shariki K, Laevsky I, Coleman R, et al. Human feeder layers for human embryonic stem cells. Biol Reprod. 2003; 68(6):2150–6. [PubMed: 12606388]
24. Levenberg S, Huang NF, Lavik E, Rogers AB, Itskovitz-Eldor J, Langer R. Differentiation of human embryonic stem cells on three-dimensional polymer scaffolds. Proc Natl Acad Sci U S A. 2003; 100(22):12741–6. [PubMed: 14561891]
25. Adewumi O, Aflatoonian B, Ahrlund-Richter L, Amit M, Andrews PW, Beighton G, et al. Characterization of human embryonic stem cell lines by the International Stem Cell Initiative. Nat Biotechnol. 2007; 25(7):803–16. [PubMed: 17572666]
26. Abramoff MD, Magalhaes PJ, Ram SJ. Image Processing with ImageJ. Biophotonics International. 2004; 11(7):36–42.
27. Levental I, Georges PC, Janmey PA. Soft biological materials and their impact on cell function. Soft Matter. 2007; 3(3):299–306.
28. Evans ND, Minelli C, Gentleman E, LaPointe V, Patankar SN, Kallivretaki M, et al. Substrate stiffness affects early differentiation events in embryonic stem cells. Eur Cell Mater. 2009; 18:1–13. discussion 13–4. [PubMed: 19768669]
29. Buxboim A, Rajagopal K, Brown AE, Discher DE. How deeply cells feel: methods for thin gels. J Phys Condens Matter. 22(19):194116. [PubMed: 20454525]
30. Foty RA, Pfleger CM, Forgacs G, Steinberg MS. Surface tensions of embryonic tissues predict their mutual envelopment behavior. Development. 1996; 122(5):1611–20. [PubMed: 8625847]
31. Wada T, Honda M, Minami I, Tooi N, Amagai Y, Nakatsuji N, et al. Highly efficient differentiation and enrichment of spinal motor neurons derived from human and monkey embryonic stem cells. PLoS One. 2009; 4(8):e6722. [PubMed: 19701462]
32. Denham M, Dottori M. Signals involved in neural differentiation of human embryonic stem cells. Neurosignals. 2009; 17(4):234–41. [PubMed: 19816060]
33. Shimosato D, Shiki M, Niwa H. Extra-embryonic endoderm cells derived from ES cells induced by GATA factors acquire the character of XEN cells. BMC Dev Biol. 2007; 7:80. [PubMed: 17605826]
34. Murray P, Edgar D. Regulation of the differentiation and behaviour of extra-embryonic endodermal cells by basement membranes. J Cell Sci. 2001; 114(Pt 5):931–9. [PubMed: 11181176]
35. D'Amour KA, Agulnick AD, Eliazer S, Kelly OG, Kroon E, Baetge EE. Efficient differentiation of human embryonic stem cells to definitive endoderm. Nat Biotechnol. 2005; 23(12):1534–41. [PubMed: 16258519]
36. Sharon N, Benvenisty N. Mesodermal Differemtiation. Human Cell Culture. 2007; 6:129–148.

37. Ashburner M, Ball CA, Blake JA, Botstein D, Butler H, Cherry JM, et al. Gene ontology: tool for the unification of biology. The Gene Ontology Consortium. Nat Genet. 2000; 25(1):25–9. [PubMed: 10802651]
38. Mostafavi S, Ray D, Warde-Farley D, Grouios C, Morris Q. GeneMANIA: a real-time multiple association network integration algorithm for predicting gene function. Genome Biol. 2008; 9 (Suppl 1):S4. [PubMed: 18613948]
39. Shannon P, Markiel A, Ozier O, Baliga NS, Wang JT, Ramage D, et al. Cytoscape: a software environment for integrated models of biomolecular interaction networks. Genome Res. 2003; 13(11):2498–504. [PubMed: 14597658]
40. Maere S, Heymans K, Kuiper M. BiNGO: a Cytoscape plugin to assess overrepresentation of gene ontology categories in biological networks. Bioinformatics. 2005; 21(16):3448–9. [PubMed: 15972284]
41. Discher DE, Janmey P, Wang YL. Tissue cells feel and respond to the stiffness of their substrate. Science. 2005; 310(5751):1139–43. [PubMed: 16293750]
42. Tao Q, Nandadasa S, McCrea PD, Heasman J, Wylie C. G-protein-coupled signals control cortical actin assembly by controlling cadherin expression in the early Xenopus embryo. Development. 2007; 134(14):2651–61. [PubMed: 17567666]
43. Burdsal CA, Damsky CH, Pedersen RA. The role of E-cadherin and integrins in mesoderm differentiation and migration at the mammalian primitive streak. Development. 1993; 118(3):829–44. [PubMed: 7521282]
44. Saez A, Buguin A, Silberzan P, Ladoux B. Is the mechanical activity of epithelial cells controlled by deformations or forces? Biophys J. 2005; 89(6):L52–4. [PubMed: 16214867]
45. Krieg M, Arboleda-Estudillo Y, Puech PH, Kafer J, Graner F, Muller DJ, et al. Tensile forces govern germ-layer organization in zebrafish. Nat Cell Biol. 2008; 10(4):429–36. [PubMed: 18364700]
46. Foty RA, Steinberg MS. The differential adhesion hypothesis: a direct evaluation. Dev Biol. 2005; 278(1):255–63. [PubMed: 15649477]

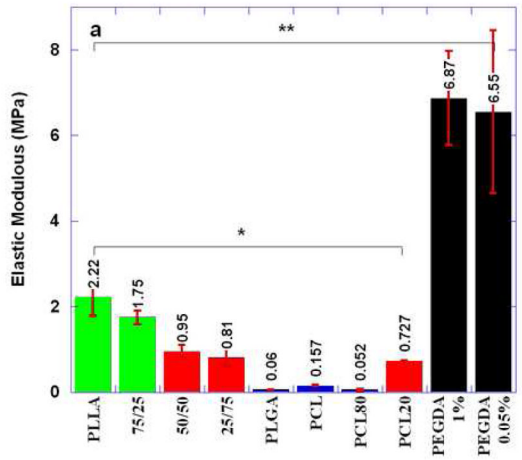

b

Scaffolds	Abbreviation	Content (w/w)	Porosity (%)
PLLA/PLGA	PLGA	0/100	90
	25/75	25/75	87
	50/50	50/50	87
	75/25	75/25	90
	PLLA	100/0	86
[PLLA/PLGA]/PCL	PCL20	[50/50]80/20	85
	PCL50	[50/50]50/50	87
	PCL80	[50/50]20/80	87
[PLLA/PLGA]/PEGDA	PEGDA 1% BP	[50/50]75/25	88
	PEGDA 0.05% BP	[50/50]75/25	85

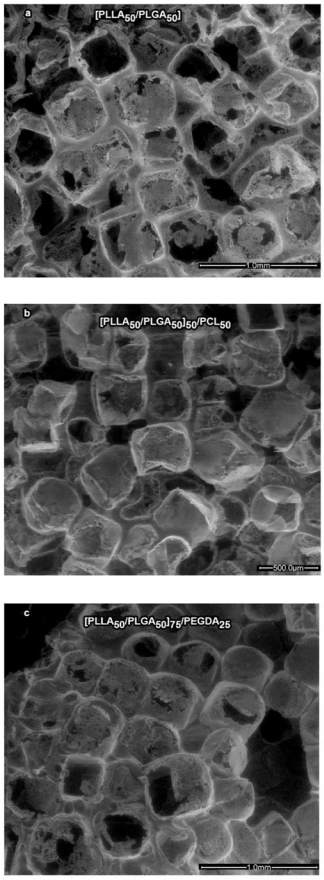

Figure 1. Scaffold composition versus elastic modulus, porosity and morphology

(a) The elastic moduli (mean ± SD, n=12) of all studied scaffolds were grouped into four color-coded categories, where columns of identical color represent moduli of significantly similar levels ($p>0.05$). Green compared to red and blue, as well as blue compared to red, present *=$p<0.05$; black compared to all others presents **=$p<0.001$. (b) Scaffold composition and porosity. (c) Representative scanning electron microscopy (SEM) micrographs of various scaffolds. Morphological analysis of these scaffolds revealed that, irrespective of chemical composition, all exhibited 85–90% porosity with interconnective open-pore morphology.

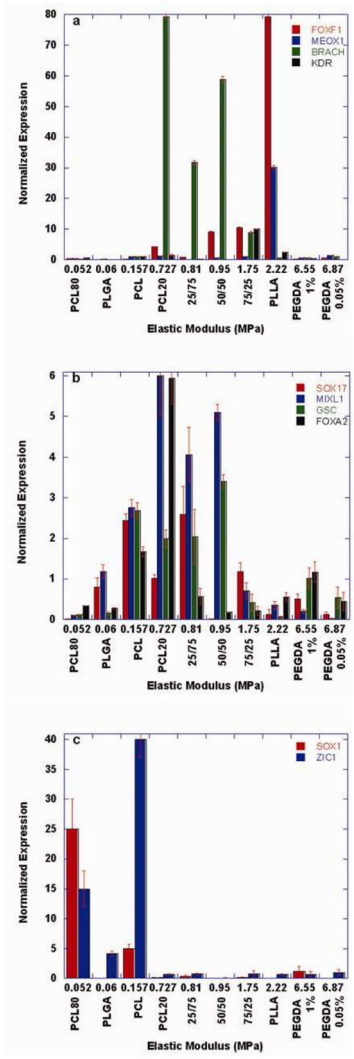

Figure 2. Effect of scaffold stiffness on hESC differentiation

After two weeks in culture, total RNA was extracted from homogenized hESC-seeded scaffolds. Expression of genes representative of the mesoderm (a), endoderm (b) and ectoderm (c) germ layers was measured by RT-PCR and normalized against GAPDH expression levels. Ratios of normalized values relative to their expression levels in suspended EBs were calculated and are presented as the mean values (±SD) of three experiments, each performed in quadruplicates.

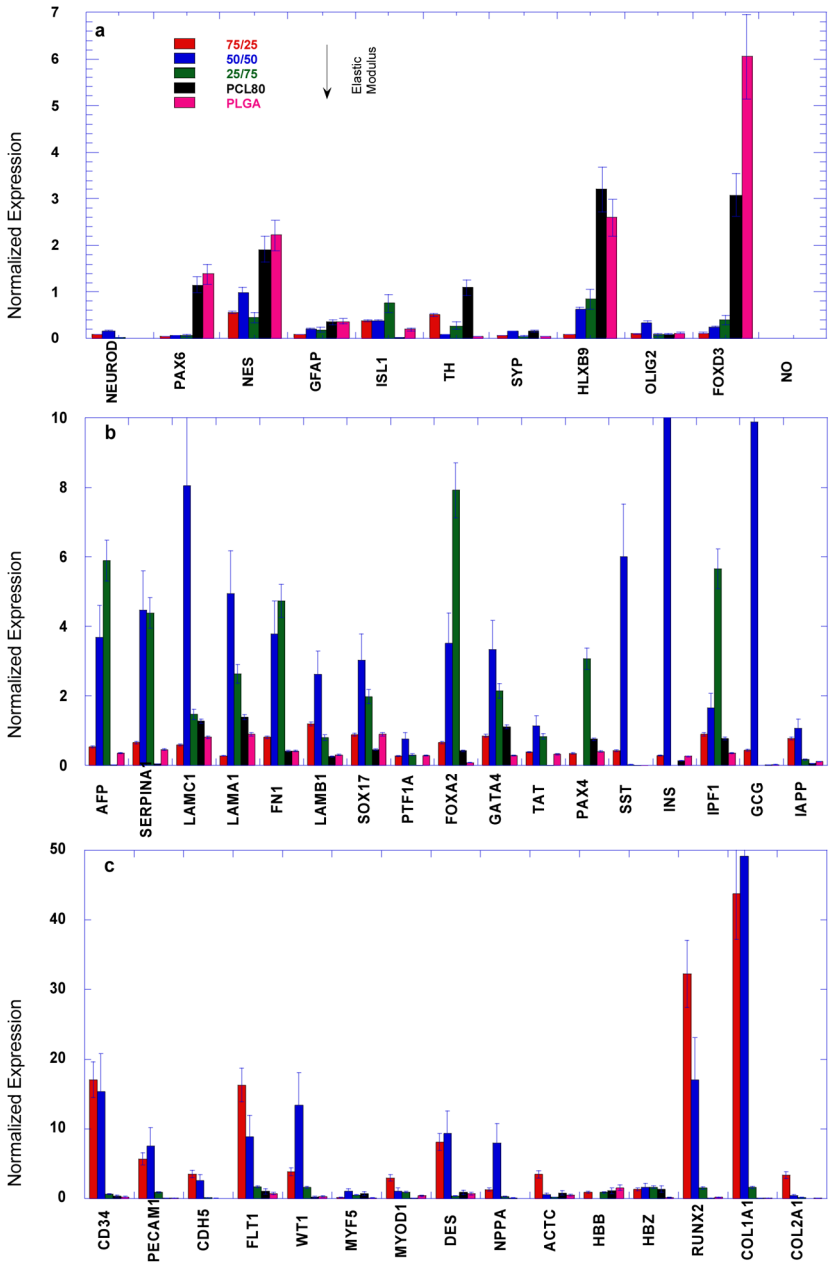

d

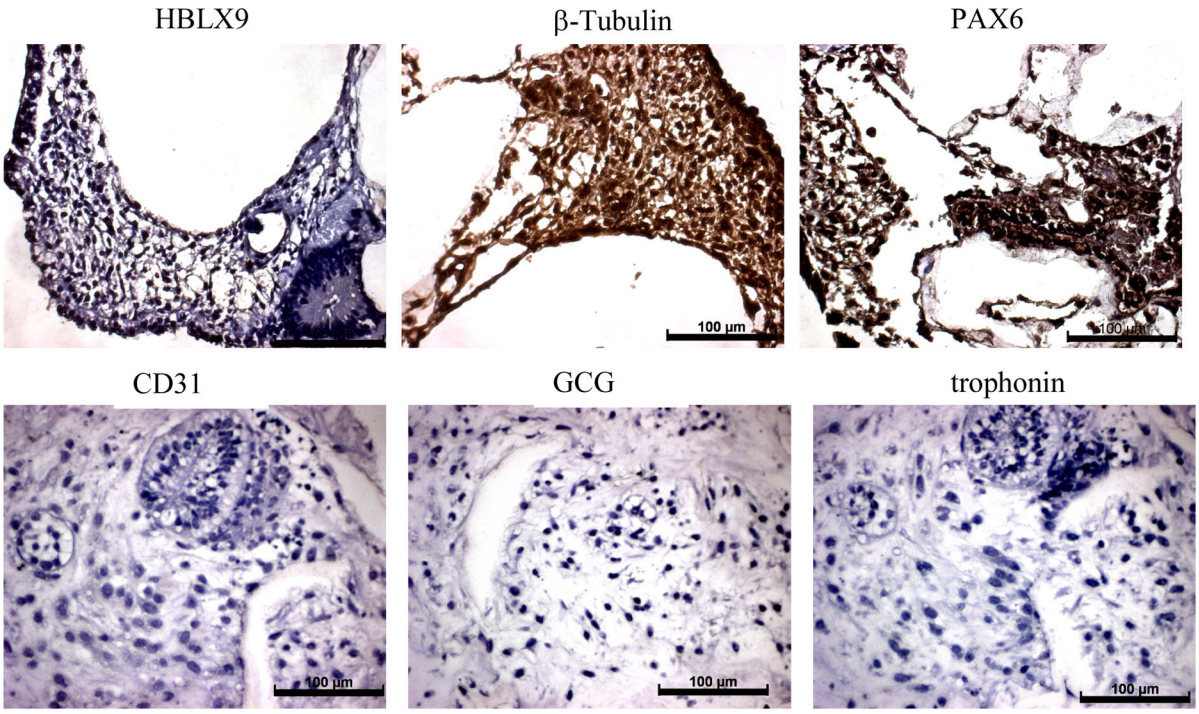

e

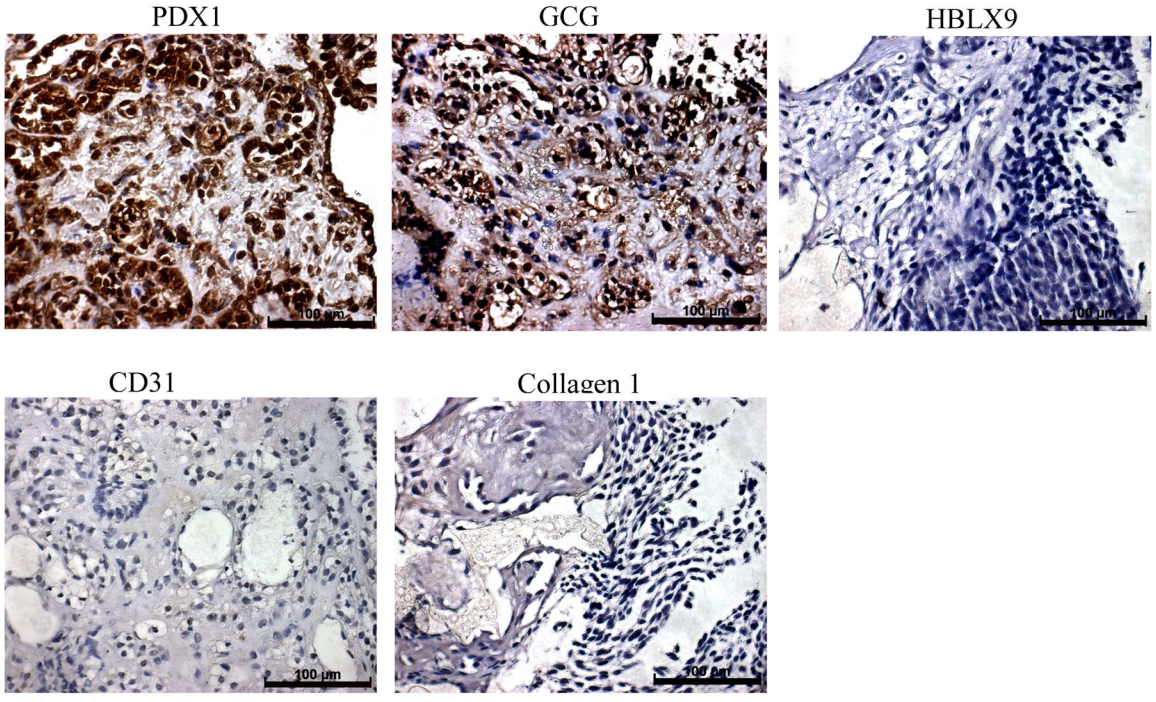

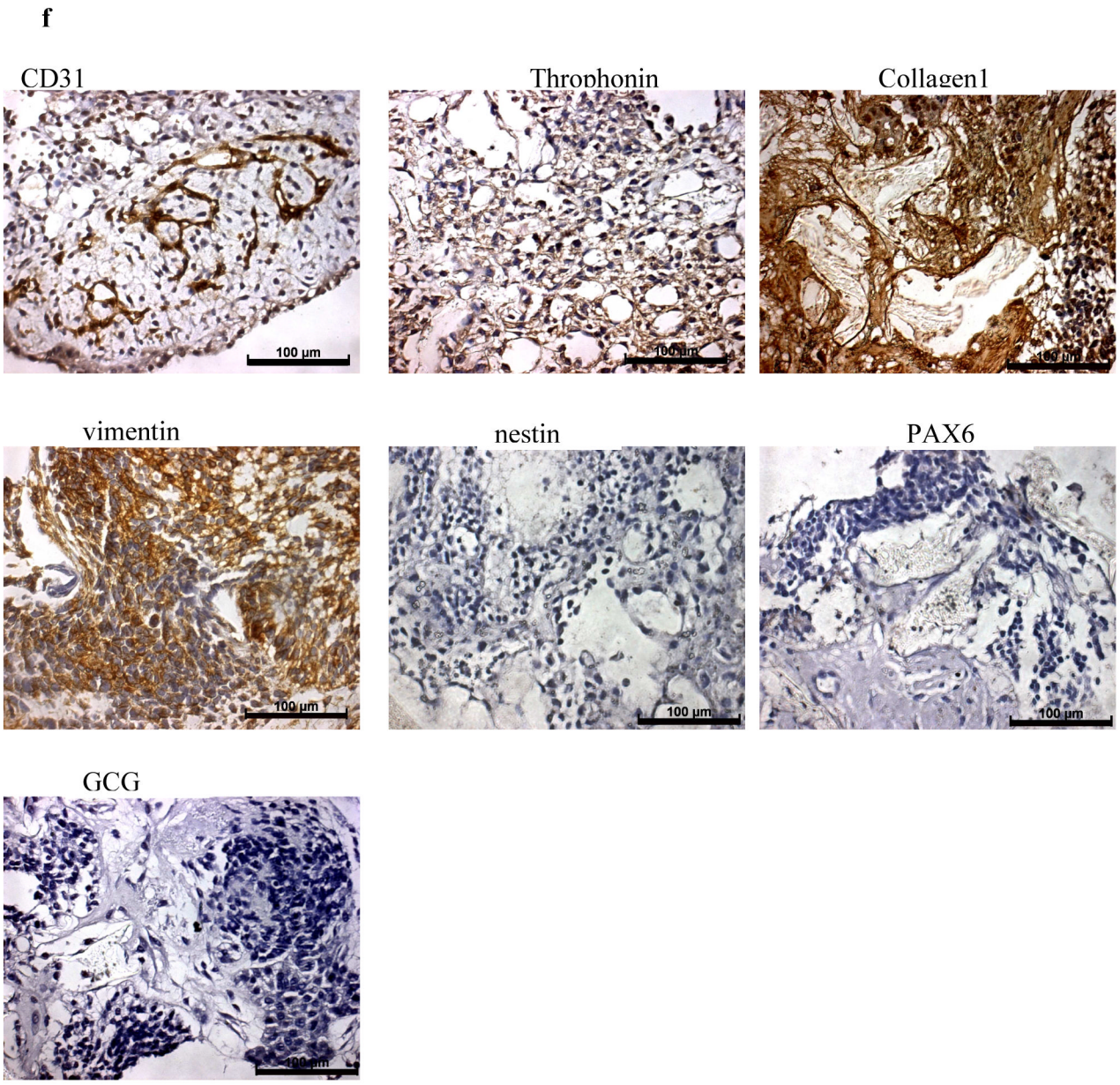

Figure 3. Differentiation of hESCs on scaffolds of varying stiffness, as determined using the Applied Biosystems hESC array

After two weeks in culture, total RNA was extracted from homogenized hESC-seeded scaffolds. Expression of selected genes representative of the mesoderm (a), endoderm (b) and ectoderm (c) germ layers was measured and are presented as described in Figure 2. Ratios are presented as mean values (±SD) of gene expression levels determined from duplicates. (d–f)Immunohystochemistry of selected mature markers expression on: (d) LoEM, (e) IntEM and (f) HiEM scaffolds.

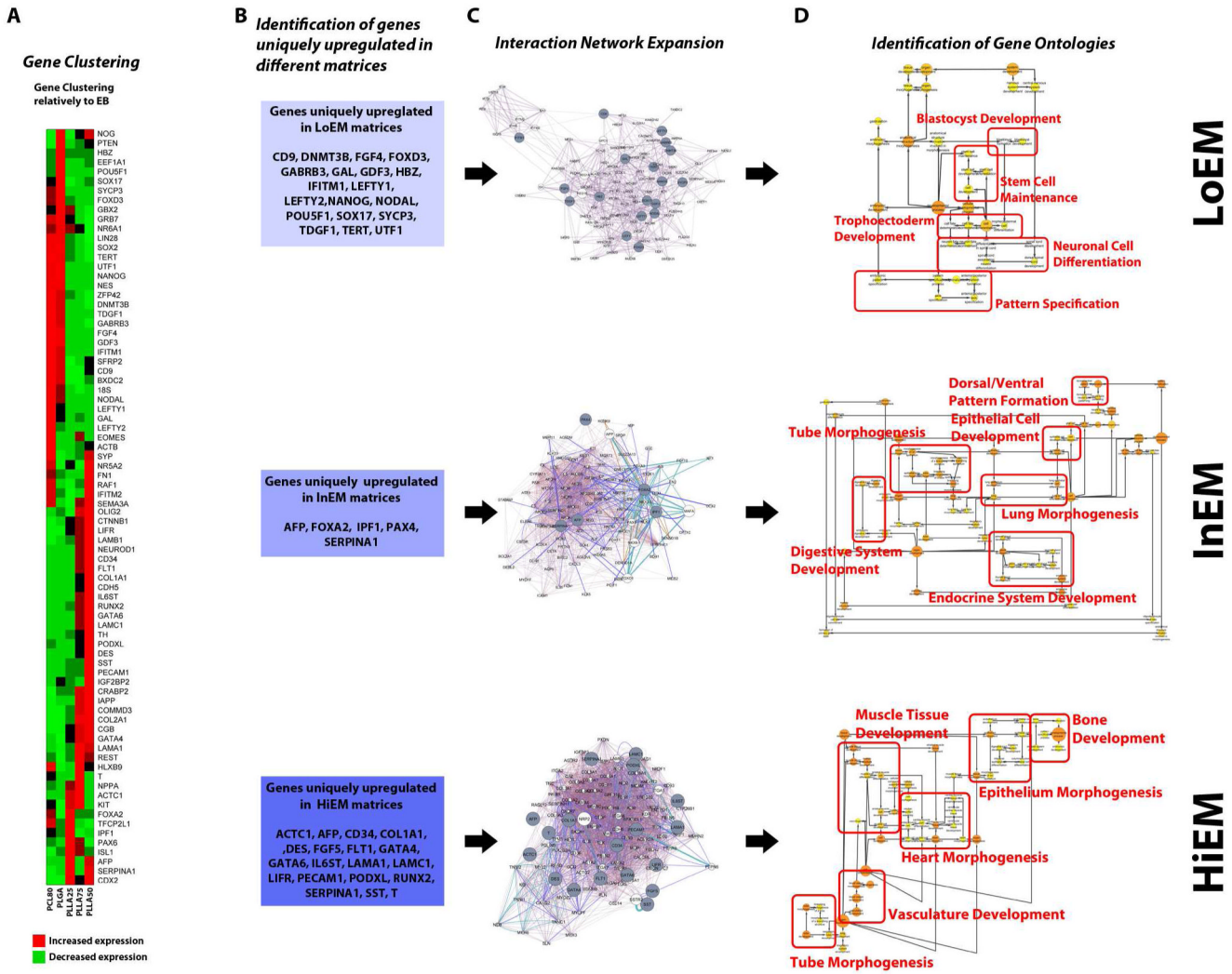

Figure 4. Differentiation of hESCs on scaffolds of varying stiffness

(a) Cluster analysis with respect to gene expression The levels of gene expression are indicated by the color change from red (high expression levels;) to green (low expression levels); (b) genes upregulated in hESC grown on the various matrices; (c) protein- protein interaction maps expanded from each upregulated gene cluster; (d) gene ontology identifying the biological processes correlating with upregulated gene clusters.

Table 1

Scaffolds	Abbreviation	Content (w/w)	Porosity (%)
PLLA/PLGA	PLGA	0/100	90
	25/75	25/75	87
	50/50	50/50	87
	75/25	75/25	90
	PLLA	100/0	86
[PLLA/PLGA]/PCL	PCL20	[50/50]80/20	85
	PCL50	[50/50]50/50	87
	PCL80	[50/50]20/80	87
[PLLA/PLGA]/PEGDA	PEGDA 1% BP	[50/50]75/25	88
	PEGDA 0.05% BP	[50/50]75/25	85